Supporting Information

A metal–phenolic nanotuner launches cancer pyroptosis for sono-immune therapy

Guohao Wang,[‡a] Dongmei Wang,[‡b] Huimin Tian,[‡c] Lu Xia,[a] Dongyan Shen,[a] Zhanxiang Wang[d] and Yunlu Dai*[e,f]*

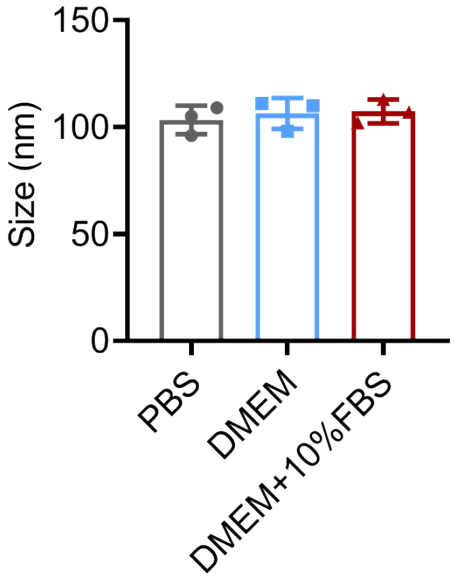

Fig. S1. Diameters of HTA NPs stored in PBS, DMEM and DMEM containing 10% of fetal bovine serum (FBS) for 3 days.

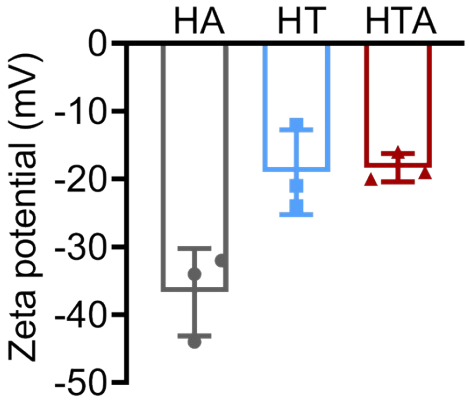

Fig. S2. Zeta potential analyses of HA, HT, and HTA NPs.

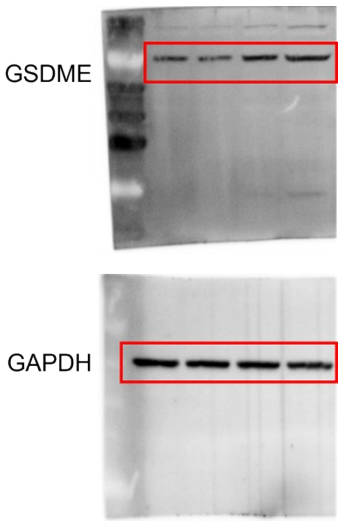

Fig. S3. The image of the full gel and blot of Fig. 2b.

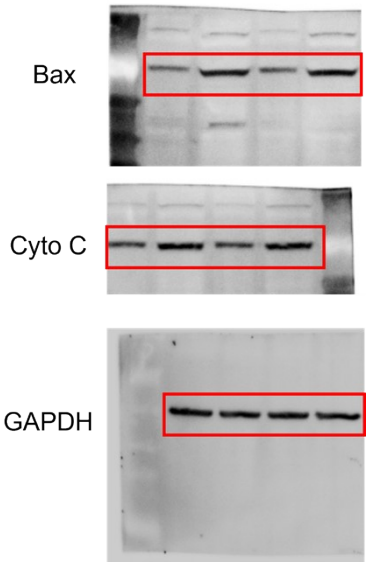

Fig. S4. The image of the full gel and blot of Fig. 3b.

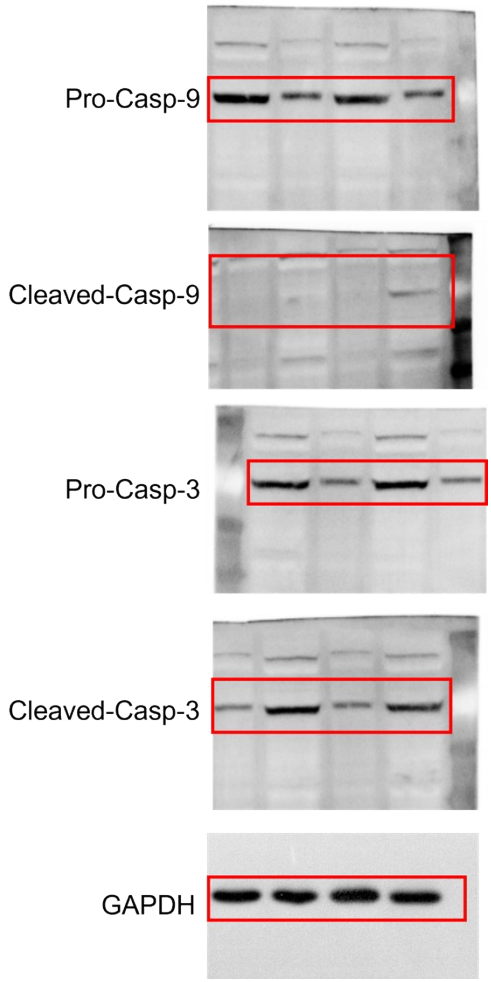

Fig. S5. The image of the full gel and blot of Fig. 3c.

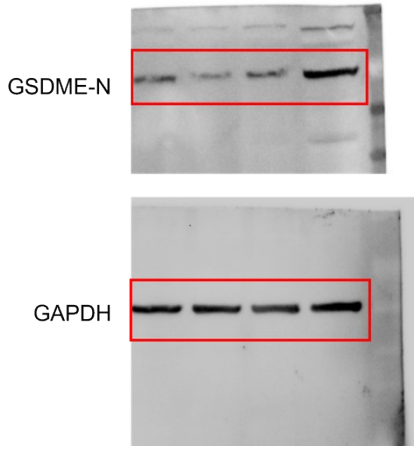

Fig. S6. The image of the full gel and blot of Fig. 3d.

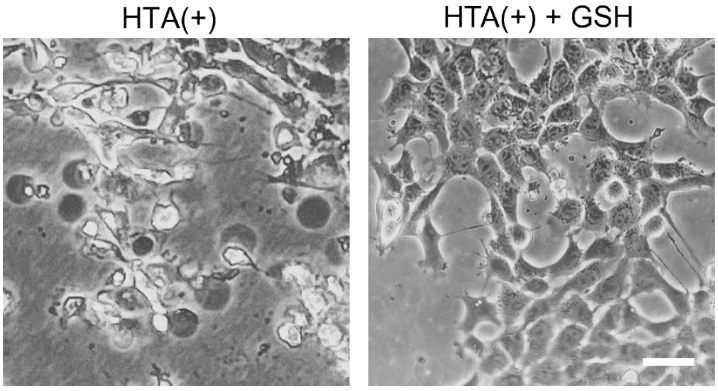

Fig. S7. GSH (glutathione), inhibitor of ROS, blocked HTA(+)-induced pyroptosis. PWE(+) for PWE plus ultrasound (1.0 MHz, 1.0 W/cm², 50% duty cycle). Scale bar: 20 μm.

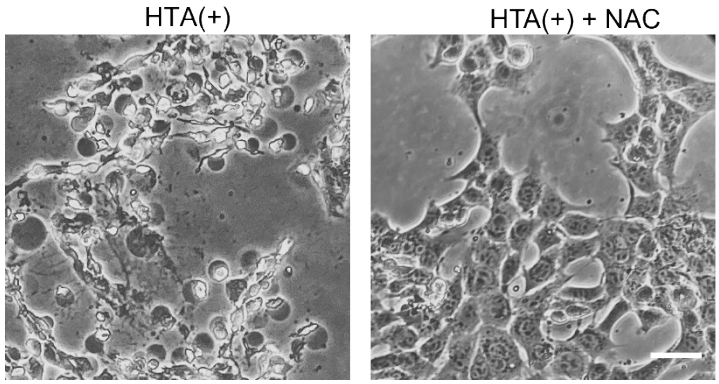

Fig. S8. NAC (N-acetyl-L-cysteine), inhibitor of ROS, HTA(+)-induced pyroptosis. PWE(+) for PWE plus ultrasound (1.0 MHz, 1.0 W/cm², 50% duty cycle). Scale bar: 20 μm.

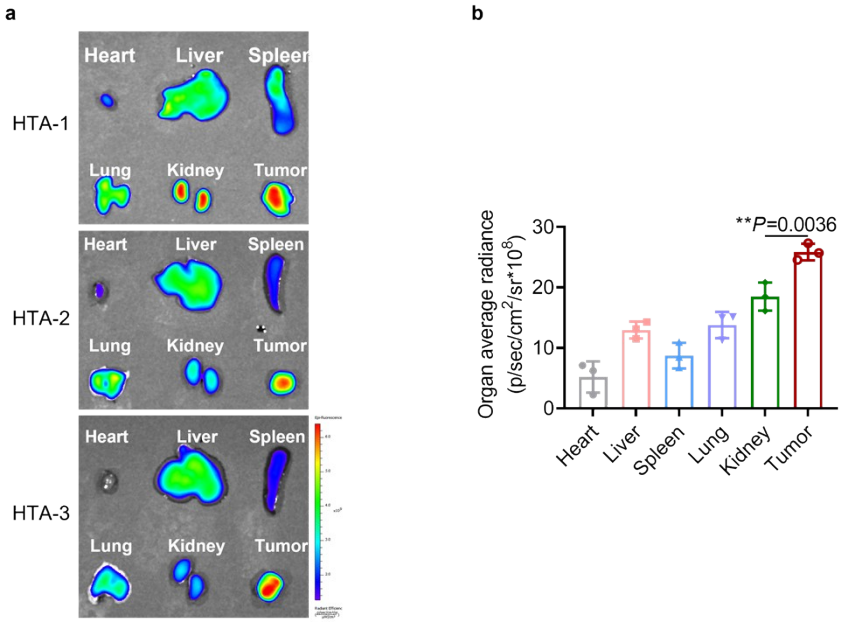

Fig. S9. Fluorescence imaging (a) and quantification of fluorescence intensity (b) in organs and tumors harvested from mice 48 hours after injection of HTA nanoparticles, which were labeled with ICG on HA-DA. The study included n = 3 biologically independent animals per group.

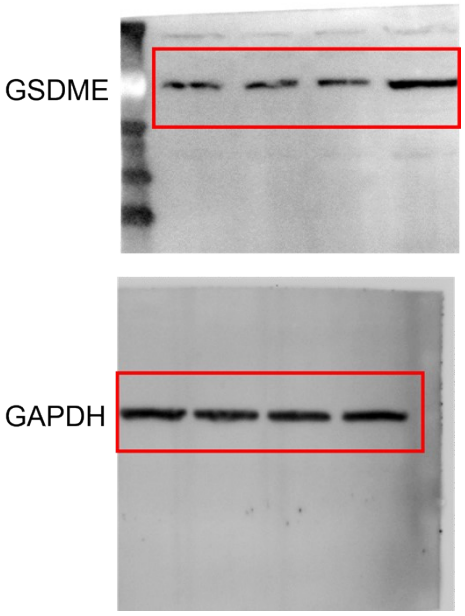

Fig. S10. The image of the full gel and blot of Fig. 4d.

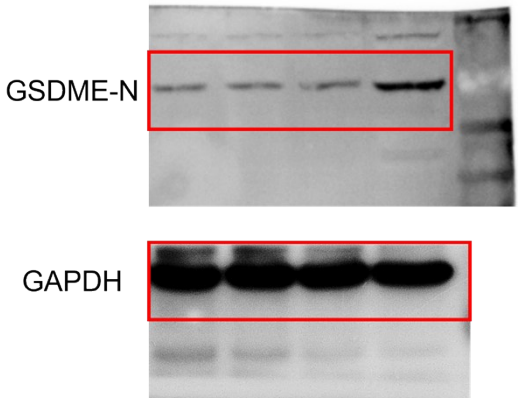

Fig. S11. The image of the full gel and blot of Fig. 4f.

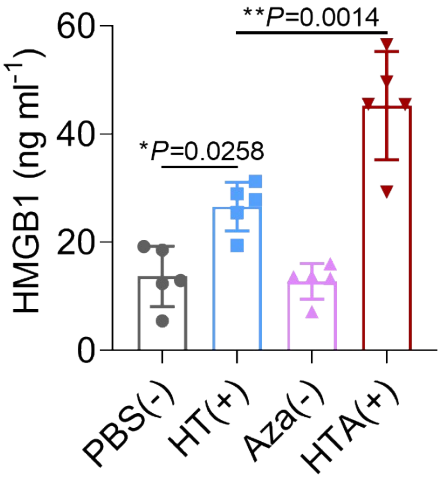

Fig. S12. HMGB1 levels in the supernatants of 4T1 cells after different treatments. (n = 5)

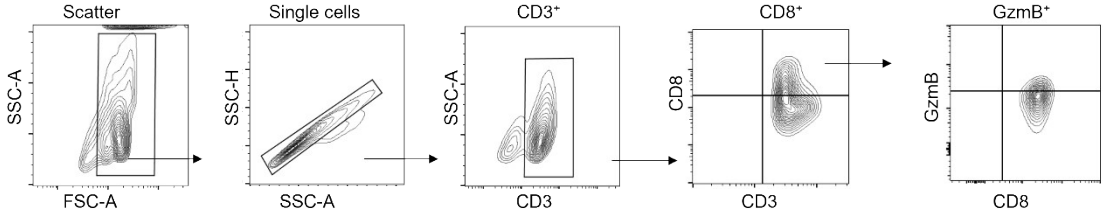

Fig. S13. Flow cytometry gating strategies for $CD3^+CD8^+$ and $CD3^+CD8^+GzmB^+$ T cells panel in TDLN.

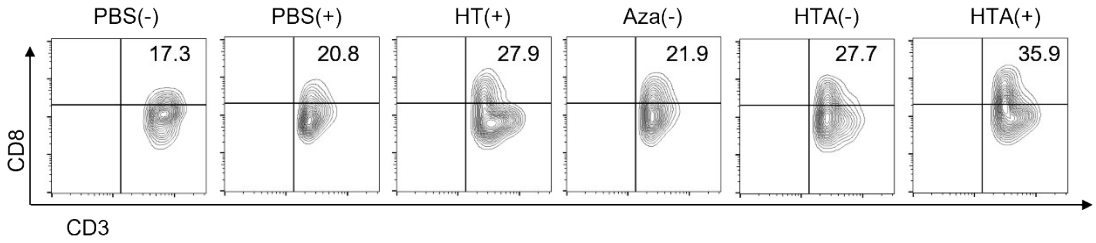

Fig. S14. Flow cytometric plots of $CD3^+CD8^+$ T cells collected from TDLN.

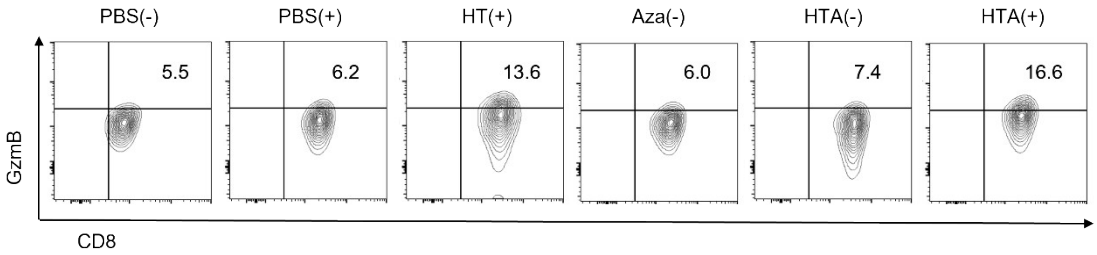

Fig. S15. Flow cytometric plots of $CD8^+$ T cells expressing granzyme B^+ collected from TDLN.

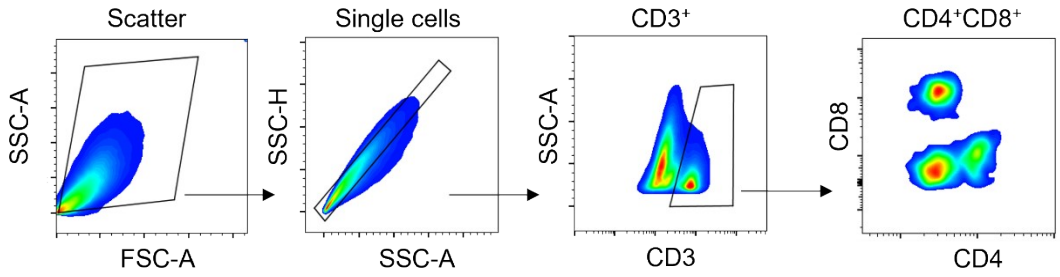

Fig. S16. Representative flow cytometry gating strategies for $CD3^+CD4^+$ and $CD3^+CD8^+$ T cells in distant tumor tissue.

Table S1. Ti^{IV} Loading efficiency in HTA

HA-DA: TiO_2: Aza (w/w)	Ti^{IV} Loading content (wt %)	Loading efficiency (%)
30:1:1	1.96	62.72
30:5:1	11.86	85.39
30:10:1	13.65	55.97

Table S2. Aza Loading efficiency in HTA

HA-DA: TiO_2: Aza (w/w)	Aza Loading content (wt %)	Loading efficiency (%)
30:1:1	2.27	72.64
30:5:1	2.43	87.48
30:10:1	2.16	88.56